



Preparation and characterization of Al doped ZnO NPs/graphene nanocomposites synthesized by a facile one-step solvothermal method

S. Asghar Khayatian^a, Ahmad Kompany^{a,*}, Nasser Shahtahmassebi^a, A. Khorsand Zak^b

^aMaterials and Electroceramics Laboratory, Department of Physics, Faculty of Science, Ferdowsi University of Mashhad, Mashhad, Iran

^bNanotechnology Laboratory, Esfarayen University of Technology, North Khorasan, Iran

Received 21 July 2015; received in revised form 3 August 2015; accepted 3 August 2015

Available online 3 September 2015

Abstract

Aluminum doped ZnO nanoparticles (AZO-NPs)/graphene nanocomposites, with different Al concentrations, were successfully synthesized by a facile one-step solvothermal method at low temperature. SEM and TEM images of the prepared samples indicated that AZO-NPs have been grown and rather well distributed on the surface of graphene sheets. The average particle size of AZO-NPs was found to decrease with increasing Al concentration. The XRD analysis confirmed the formation of AZO-NPs/graphene nanocomposites with hexagonal wurtzite structure. The results of FT-IR and Raman spectroscopy showed that the oxygen-containing groups, which exist on the surface of the graphene oxide sheets, are removed and the graphene oxide is reduced to graphene during the synthesis procedure. Our results revealed that the simple low cost method used in this work is suitable for the synthesis of graphene-based semiconductor nanocomposites.

© 2015 Elsevier Ltd and Techna Group S.r.l. All rights reserved.

Keywords: B. Nanocomposite; Graphene oxide; Solvothermal; AZO nanoparticles

1. Introduction

Nowadays, one of the main purposes of nanoscience is to synthesize materials with enhanced properties. There are several parameters which affect the properties of nanostructured materials including (I) the technique used for preparation, (II) control the synthesis conditions, (III) tuning the distribution of atoms and (IV) incorporation of dopant atoms into the lattice of nanostructure [1,2]. Among nano-scale materials, semiconductor nanostructures have attracted much attention due to their unique properties and are used widely in different branches of science and technology. Zinc oxide (ZnO) as a large energy band gap (3.37 eV) semiconductor at room temperature and the exciton binding energy of about 60 meV has found many applications [3]. Furthermore, the properties and applications of ZnO depend strongly on its morphology and the particle size [4,5]. For example, ZnO with various

structures such as nanowires and nanoparticles have been used in different applications including gas sensors [6], solar cells [7] and as photocatalytic materials [8]. In order to modify the physical properties of the semiconductor nanostructures, doping is an effective way. Doping ZnO with certain elements such as Sn, Ga, In, Mn, Mg, Bi, and Co affects its crystal growth and optical and electrical properties [9–13]. Yang et al. [14] doped Co^{2+} into ZnO structure which reduced its energy band gap from 3.11 eV to 2.83 eV. Lim et al. [15], have reported that the substitution of Zn^{2+} with Ga^{3+} improves the electrical conductivity of ZnO, due to the increase of charge carrier concentration. In comparison with bulk zinc oxide, ZnO nanoparticles show better optical properties due to the quantum confinement [16]. Usually, semiconductor nanoparticles agglomerate during the preparation procedure because of their high surface energy, resulting in surface to volume ratio decrease. These agglomerated nanoparticles are not suitable to be used as photo-adsorption materials [17]. Graphene, as a two-dimensional carbon nanomaterial, has excellent mechanical, structural and electrical properties. Moreover, the specific

*Corresponding author.

E-mail address: kompany@um.ac.ir (A. Kompany).

surface area of graphene is about $2630 \text{ m}^2 \text{ g}^{-1}$, which makes it a good supporting material for dispersing the semiconductor nanoparticles [18]. Many attempts have been made to load various nanoparticles such as TiO_2 [19], Fe_3O_4 [20] and CuO [21] on the surface of graphene sheets with uniform distribution. It seems, decorating graphene by semiconductor nanoparticles not only prevents the agglomeration of the particles but also, implies new physical and chemical properties in the graphene-based semiconductor nanomaterials. Up to our knowledge, there is no records on the synthesis and the detailed structural analysis of Al doped ZnO NPs/graphene nanocomposites in the literatures. In this work, a facile and nontoxic route for the synthesis of AZO-NPs/graphene nanocomposite is presented and the effects of Al concentration on the structural and optical properties of the prepared nanocomposites were investigated.

2. Experimental procedure

2.1. Synthesis of graphene oxide sheets (GOs)

The modified Hummer method was used to prepare the graphene oxide sheets (GOs) [22]. Briefly, certain amounts of natural graphite powder (1 g), sodium nitrate (0.5 g) and 23 ml of concentrated H_2SO_4 were put in a 500 ml beaker placed in the ice-bath. Then 3 g of KMnO_4 was added gradually, while stirring and keeping the temperature at about 10°C . The resulting mixture was stirred for another 2 h at 35°C and then diluted with 46 ml deionized water (DI). The addition of water to the solution caused the temperature increase up to 100°C . Now, 140 ml DI was used to further dilatation of the solution and then 10 ml H_2O_2 (30%) was added in order to reduce the

residual KMnO_4 so that the color of the solution changed into brilliant yellow. finally, the obtained mixture was centrifuged and washed with 5% HCl solution and DI several times and then dried at 60°C for 24 h.

2.2. Preparation of AZO-NPs/graphene nanocomposites

In order to prepare Al doped ZnO NPs/graphene nanocomposite, 20 mg of GOs was dispersed in 80 ml of ethylene glycol (EG) in a bath sonicator for 1 h. After that, 80 mg of zinc nitrate hexahydrate ($\text{Zn}(\text{NO}_3)_2 \cdot 6\text{H}_2\text{O}$, 98% Sigma-Aldrich) and different weight percent (1, 3 and 5 wt%) of aluminum nitrate nine hydrate ($(\text{Al}(\text{NO}_3)_3 \cdot 9\text{H}_2\text{O})$, $\geq 98\%$ Sigma-Aldrich) were dissolved in 80 ml of EG. Also, 20 mg of NaOH was dissolved in 20 ml of DI water, added to the prepared solution. The resulting solution was transferred into a 200 ml Teflon-lined stainless steel autoclave which was kept for 24 h at 160°C . The final product was washed by ethanol and DI water and then dried for 24 h in an oven at 80°C .

2.3. Characterization

The synthesized samples were characterized using scanning electron microscopy (SEM, LeO-VP1450-Germany), atomic force microscopy (AFM, Asylum Research Cypher), X-ray diffraction (XRD-6000, Shimadzu, Japan) with $\text{Cu K}\alpha$ radiation ($\lambda = 1.54056 \text{ \AA}$) and transmission electron microscopy (TEM, LeO-912AB- Germany). Also, energy dispersive X-ray (EDX) spectroscopy was performed for elemental investigation of the prepared samples. Fourier transform infrared (FT-IR) and Raman spectroscopy were carried out to study the reduction of GOs to graphene.

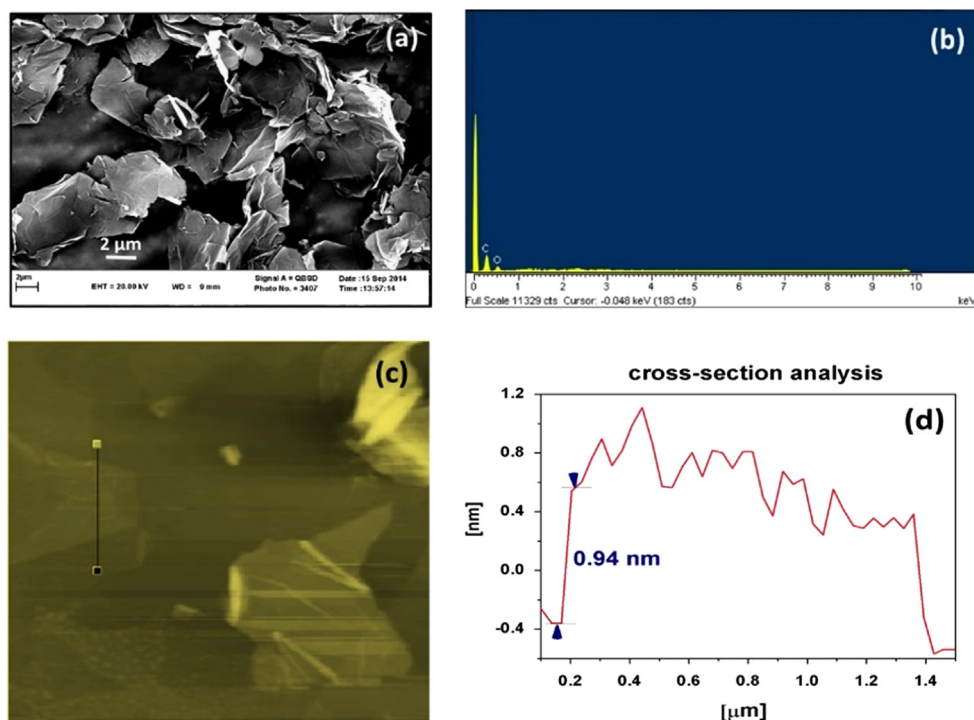


Fig. 1. (a) SEM image and (b) EDX analysis of GOs, (c) AFM image and (d) the corresponding cross-section analysis of GO sheet.

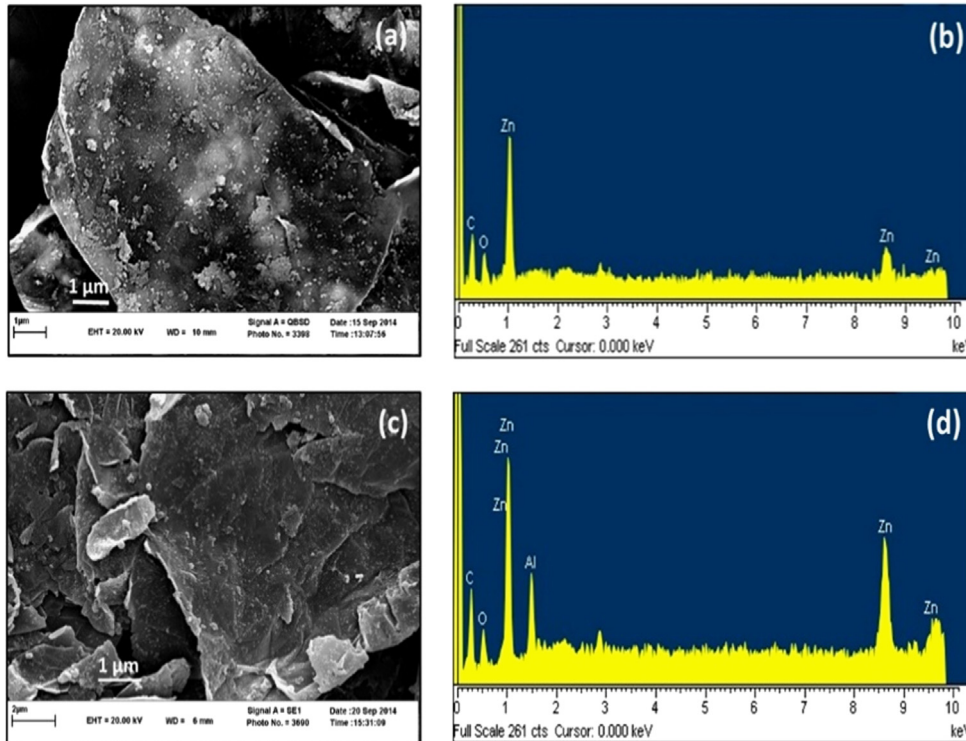


Fig. 2. SEM images of (a) ZnO-NPs/graphene, (c) 3% AZO-NPs/graphene nanocomposite and (b,d) their EDX analyses.

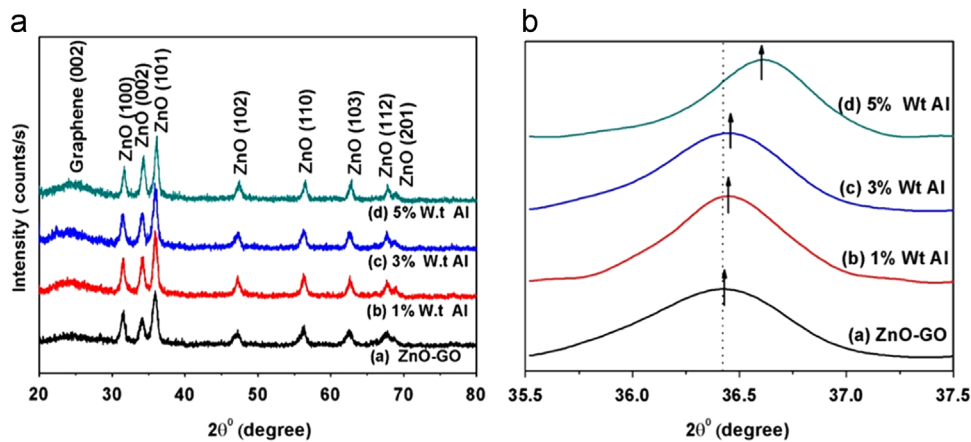


Fig. 3. (A) XRD patterns of ZnO-NPs/graphene and AZO-NPs/graphene with different Al concentrations and (B) (101) peak of XRD patterns.

3. Results and discussion

The SEM image and EDX spectrum of the prepared GOs are shown in Fig. 1(a) and (b). Fig. 1(a) shows that GOs surface are very neat, but rather folded. The EDX analysis, Fig. 1(b), confirms the existence of only C and O elements in the prepared samples. Fig. 1(c) and (d) are the AFM image and the cross-section analysis of the GOs, respectively, which reveal that the graphene oxide sheets have been produced and the thickness of a typical layer is about 0.94 nm which is slightly greater than the value reported theoretically for single-layer graphene (0.78 nm) [23]. This difference in the thickness is due to the presence of the functional groups such as epoxides,

carbonyl, carboxyl and hydroxyl radicals on the surface of the prepared GOs [24,25]. Fig. 2 indicates the SEM images and EDX spectra of the ZnO-NPs/graphene and 3% Al doped ZnO-NPs/graphene nanocomposites. As shown in Fig. 2a and c, the undoped and Al doped ZnO-NPs have been grown on GOs because of the presence of the functional groups on the surface of GOs which act as anchoring sites and also, preventing the agglomeration of the nanoparticles. In addition, the existence of ZnO and AZO-NPs forbid the graphene oxide sheets from sticking to each other, so they play as stabilizer agents. The EDX spectra of ZnO-NPs/graphene and AZO-NPs/graphene nanocomposites, presented in Fig. 2(b) and (d), confirm the existence of Zn, O, C and Al elements in the prepared samples. The XRD spectra of the synthesized ZnO-

NPs/graphene and AZO-NPs/graphene samples are shown in Fig. 3. These spectra indicate that all the samples have wurtzite structure in accordance with JCPDS card No. 36-1451 and also are quite pure [13,26]. In comparison with the pure ZnO peaks [27], the intensity of the major diffraction peaks decreases in the prepared ZnO-NPs/graphene and AZO-NPs/graphene nanocomposites with increasing Al concentration. This result can be related to the presence of graphene and Al dopants, indicating that the size of the ZnO, AZO-NPs and also their crystallite quality have decreased. Also, there is no additional peak corresponding to Al reflection peak in XRD patterns of the synthesized samples, which indicates the exciting of Al^{3+} ions in ZnO lattice prohibiting the formation of the hydroxide phase [27]. Moreover, the small hump which is seen in all patterns, at around $2\theta=24.50^\circ$, is assigned to graphene layers [28]. It can be observed in Fig. 3(B), the negligible changes in the position of the peaks, for example the position of (101) peak, toward higher 2θ takes place by increasing of Al concentration. This shift can be attributed to the difference in ionic radii of Zn^{2+} (0.74 Å) and Al^{3+} (0.53 Å), resulting in the decrease of the inter-planar spacing of AZO-NPs in the nanocomposites [29]. The TEM images of the prepared samples are shown in Fig. 4(a) and (b) which shows that the surface of the graphene layers are decorated by ZnO-NPs and AZO-NPs, respectively. The histogram of the particles distribution are given in Fig. 4(c) and (d). The average particle size of ZnO-NPs and 3% AZO-NPs on the graphene sheets are

21.29 ± 1 and 19.94 ± 1 nm, respectively. It is believed that some Al atoms are placed near the boundary of ZnO-NPs, which results in terminating the growth rate of AZO-NPs. Similar behavior has been reported in the literature [26,30]. The presence of the functional groups on GOs causes the electronegativity of the graphene oxide sheets to increase. Therefore, when Zn^{2+} ions are replaced by Al^{3+} in ZnO lattice, each Al^{3+} adds one electron to the lattice and this electron is capable to make a bond with a functional group on GOs through electrostatic interaction. Fig. 5 presents the FT-IR and Raman spectra of the prepared GO, ZnO-NPs/graphene and 3% AZO-NPs/graphene samples. In the FT-IR spectrum of GO, Fig. 5(A-a), there are a wide region absorption band around 3445 cm^{-1} and a narrow band at 1615 cm^{-1} , which are related to the hydroxyl stretching vibrations of C–OH groups. The bands at 1732 cm^{-1} and 1050 cm^{-1} are attributed to C=O and C–O–C groups, respectively. The band at about 1221 cm^{-1} is assigned to O–H due to the deformation of C–OH groups [31]. As reported previously, ZnO-NPs have an absorption band at about 440 cm^{-1} and a shoulder at 500 cm^{-1} in its FT-IR spectrum which are related to E_2 mode of wurtzite structure and the existence of oxygen deficiency in its lattice, respectively. These peaks are shown in ZnO-NPs/graphene spectrum, Fig. 5(A-b), indicating the existence of ZnO-NPs on the graphene sheets. Compared to the spectrum of GO shown in Fig. 5(A-a), the peak related to C–O–C has almost disappeared and the intensity of the peak corresponding

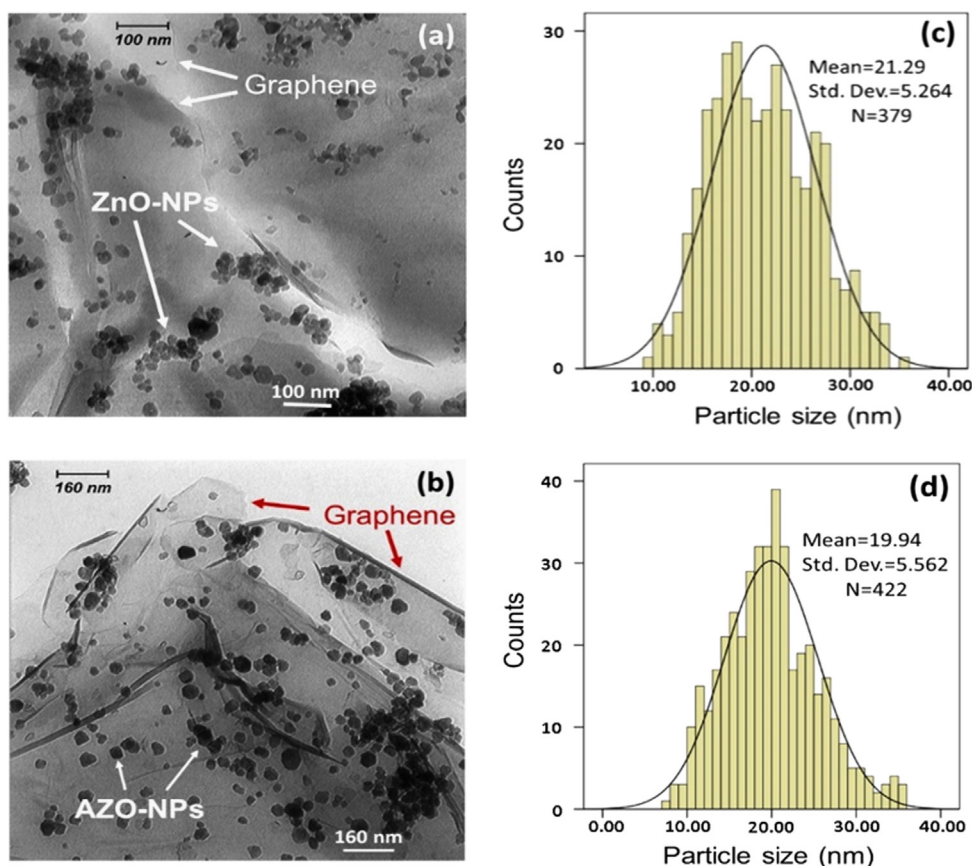


Fig. 4. TEM images of (a) ZnO-NPs/graphene, (b) 3% AZO-NPs/graphene nanocomposites and (c, d) corresponding histograms.

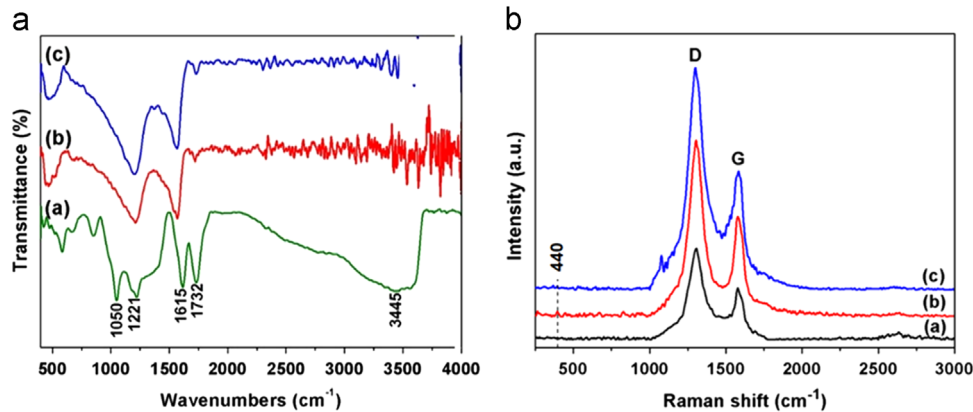


Fig. 5. (A) FT-IR and (B) Raman spectra of (a) GO, (b) ZnO-NPs/graphene and (c) 3% AZO-NPs/graphene.

to C=O has weakened in spectra of ZnO-NPs/graphene and also AZO-NPs/graphene nanocomposites, Fig. 5(A-b) and (A-c). these results confirm that the graphene oxide has been reduced to graphene during the synthesis of the nanocomposites [32]. As shown in Fig. 5(A-c), there is a peak at around 683 cm^{-1} , corresponding to Al–O stretching mode. Also, as it can be seen in this figure the shoulder related to oxygen vacancies in ZnO lattice has disappeared [2,33]. This result offers that the Al dopants have caused the decrease of oxygen deficiency and also added additional electrons into the structure [34]. Raman spectroscopy is widely used to study the quality of the crystallite structure of the carbonaceous materials. Fig. 5(B) shows the Raman spectra of the prepared samples. In Fig. 5(B-a), there are two peaks at about 1363 cm^{-1} and 1594 cm^{-1} which correspond to D and G bands related to GO, respectively [35]. According to earlier publications, ZnO has a strong peak at about 438 cm^{-1} and several peaks from 380 to 580 cm^{-1} which are attributed to the first-order optical E_2 mode of wurtzite structure [36]. In order to ZnO-NPs/graphene nanocomposite to be formed, Zn^{2+} ions are adsorbed on the surface of GO due to the presence of the functional groups via electrostatic attraction which act as nuclei centers for the growth of ZnO nanoparticles. Therefore, a bond between Zn, O and carbon atom of graphene (Zn–O–C) will be created causing the extension of Zn–O bond length which in turn results in the decrease of E_2 mode intensity of ZnO. The presence of Al^{3+} ions into ZnO lattice increases the stress of AZO lattice and also weakens the peak of E_2 mode, due to the ionic radii difference of Zn^{2+} and Al^{3+} , Fig. 5(B-c). It can be seen in Fig. 5(B-c) that there is a peak at about 1072 cm^{-1} which is related to the combination of vibrational modes of the transverse and longitudinal optical phonons [37]. The intensity ratio of D and G bands (I_D/I_G) was used to determine the disorder degree and the average size of sp^2 domains of the samples. This was obtained 1.760, 1.761 and 1.869 for GO, ZnO-NPs/graphene and 3% AZO-NPs/graphene nanocomposites, respectively. The increase of I_D/I_G ratio shows that the size of sp^2 domains and the number of oxygen-containing groups on GO have decrease resulting in the increase of superficial defects. These defects act as nuclei centers for growing the nanoparticles and also cause the almost

Table 1
Raman data obtained for GO, ZnO-NPs/graphene and 3% AZO-NPs/graphene nanocomposites.

samples	D band position (cm^{-1})	G band position (cm^{-1})	I_D	I_G	I_D/I_G
GO	1306	1578	118.90	67.519	1.760
ZnO-NPs/graphene	1304.5	1577.5	230.501	130.818	1.761
3% AZO-NPs/graphene	1300.5	1573.5	290.727	155.469	1.869

uniform distribution of nanoparticles on the surface of the graphene sheets. The Raman spectroscopy results are summarized in Table 1.

4. Conclusion

Graphene-based Al doped ZnO nanocomposites (AZO-NPs/graphene) were synthesized by a facile one-step solvothermal method with different Al concentrations. SEM, TEM and XRD results indicated that the undoped and Al doped ZnO-NPs have been loaded on the graphene sheets with wurtzite hexagonal phase. Also, FT-IR and Raman spectra revealed the reduction of graphene oxide to graphene leading to the creation of more defects on the graphene sheets. Moreover, our results indicated that doping ZnO by Al results in the decrease of nanoparticles. It can be concluded that the prepared AZO-NPs/graphene nanocomposites can be a good candidate for using in fabricating devices which need the high adsorption.

References

- [1] S.Y. Bae, C.W. Na, J.H. Kang, J. Park, Comparative structure and optical properties of Ga-, In-, and Sn-doped ZnO nanowires synthesized via thermal evaporation, *J. Phys. Chem. B* 109 (2005) 2526–2531.
- [2] N.R. Yogamalar, A. Chandra Bose, Absorption–emission study of hydrothermally grown Al:ZnO nanostructures, *J. Alloy. Compd.* 509 (2011) 8493–8500.
- [3] D. Jung, Syntheses and characterizations of transition metal-doped ZnO, *Solid State Sci.* 12 (2010) 466–470.
- [4] Y. Li, J. Meng, Al-doping effects on structure and optical properties of ZnO nanostructures, *Mater. Lett.* 117 (2014) 260–262.

- [5] N. Kiamarsipour, R. Shoja Razavi, Characterization and optical property of ZnO nano-, submicro- and microrods synthesized by hydrothermal method on a large-scale, *Superlattices Microstruct.* 52 (2012) 704–710.
- [6] M. Hjiri, L. El Mir, S.G. Leonardi, A. Pistone, L. Mavilia, G. Neri, Al-doped ZnO for highly sensitive CO gas sensors, *Sens. Actuators B: Chem.* 196 (2014) 413–420.
- [7] A. Apostoluk, Y. Zhu, B. Masenelli, J.-J. Delaunay, M. Sibiński, K. Znajdek, A. Focsa, I. Kaliszewska, Improvement of the solar cell efficiency by the ZnO nanoparticle layer via the down-shifting effect, *Microelectron. Eng.* 127 (2014) 51–56.
- [8] R.Y. Hong, J.H. Li, L.L. Chen, D.Q. Liu, H.Z. Li, Y. Zheng, J. Ding, Synthesis, surface modification and photocatalytic property of ZnO nanoparticles, *Powder Technol.* 189 (2009) 426–432.
- [9] S. Suwanboon, P. Amornpitoksuk, A. Haidoux, J.C. Tedenac, Structural and optical properties of undoped and aluminium doped zinc oxide nanoparticles via precipitation method at low temperature, *J. Alloy. Compd.* 462 (2008) 335–339.
- [10] X. Chong, L. Li, X. Yan, D. Hu, H. Li, Y. Wang, Synthesis, characterization and room temperature photoluminescence properties of Al doped ZnO nanorods, *Phys. E: Low-Dimens. Syst. Nanostruct.* 44 (2012) 1399–1405.
- [11] A. Alkahlout, N.A. Dahoudi, I. Grobelsek, M. Jilavi, P.W.d. Oliveira, Synthesis and characterization of aluminum doped zinc oxide nanostructures via hydrothermal route, *J. Mater.* (2014).
- [12] H.Y. He, Q. Liang, Enhancement in the optical transmittance of ZnO:Al powders by Mo co-doping, *Curr. Appl. Phys.* 12 (2012) 865–869.
- [13] A. Echresh, M. Zargar Shoushtari, Synthesis of Al-doping ZnO nanoparticles via mechanochemical method and investigation of their structural and optical properties, *Mater. Lett.* 109 (2013) 88–91.
- [14] H. Yang, S. Nie, Preparation and characterization of Co-doped ZnO nanomaterials, *Mater. Chem. Phys.* 114 (2009) 279–282.
- [15] S.K. Lim, S.H. Hong, S.-H. Hwang, S. Kim, H. Park, Characterization of Ga-doped ZnO nanorods synthesized via microemulsion method, *J. Mater. Sci. Technol.* 29 (2013) 39–43.
- [16] G. Srinet, R. Kumar, V. Sajal, Effects of aluminium doping on structural and photoluminescence properties of ZnO nanoparticles, *Ceram. Int.* 40 (2014) 4025–4031.
- [17] F. Xu, Y. Yuan, D. Wu, M. Zhao, Z. Gao, K. Jiang, Synthesis of ZnO/Ag/graphene composite and its enhanced photocatalytic efficiency, *Mater. Res. Bull.* 48 (2013) 2066–2070.
- [18] T.-F. Yeh, J. Cihlár, C.-Y. Chang, C. Cheng, H. Teng, Roles of graphene oxide in photocatalytic water splitting, *Mater. Today* 16 (2013) 78–84.
- [19] D. Wang, D. Choi, J. Li, Z. Yang, Z. Nie, R. Kou, D. Hu, C. Wang, L. V. Saraf, J. Zhang, I.A. Aksay, J. Liu, Self-assembled TiO₂-graphene hybrid nanostructures for enhanced Li-ion insertion, *ACS Nano* 3 (2009) 907–914.
- [20] J.-Z. Wang, C. Zhong, D. Wexler, N.H. Idris, Z.-X. Wang, L.-Q. Chen, H.-K. Liu, Graphene-encapsulated Fe₃O₄ nanoparticles with 3D laminated structure as superior anode in lithium ion batteries, *Chem. A Eur. J.* 17 (2011) 661–667.
- [21] Y.J. Mai, X.L. Wang, J.Y. Xiang, Y.Q. Qiao, D. Zhang, C.D. Gu, J. P. Tu, CuO/graphene composite as anode materials for lithium-ion batteries, *Electrochim. Acta* 56 (2011) 2306–2311.
- [22] R.E.O. W.S. Hummers, Preparation of graphitic oxide, *Am. Chem. Soc.* 80 (1958) 1339.
- [23] X. Fan, W. Peng, Y. Li, X. Li, S. Wang, G. Zhang, F. Zhang, Deoxygenation of exfoliated graphite oxide under alkaline conditions: a green route to graphene preparation, *Adv. Mater.* 20 (2008) 4490–4493.
- [24] S. Stankovich, D.A. Dikin, R.D. Piner, K.A. Kohlhaas, A. Kleinhammes, Y. Jia, Y. Wu, S.T. Nguyen, R.S. Ruoff, Synthesis of graphene-based nanosheets via chemical reduction of exfoliated graphite oxide, *Carbon* 45 (2007) 1558–1565.
- [25] B. Li, T. Liu, Y. Wang, Z. Wang, ZnO/graphene-oxide nanocomposite with remarkably enhanced visible-light-driven photocatalytic performance, *J. Colloid Interface Sci.* 377 (2012) 114–121.
- [26] M. Ahmad, E. Ahmed, Y. Zhang, N.R. Khalid, J. Xu, M. Ullah, Z. Hong, Preparation of highly efficient Al-doped ZnO photocatalyst by combustion synthesis, *Curr. Appl. Phys.* 13 (2013) 697–704.
- [27] S.-S. Lo, D. Huang, C.H. Tu, C.-H. Hou, C.-C. Chen, Raman scattering and band-gap variations of Al-doped ZnO nanoparticles synthesized by a chemical colloid process, *J. Phys. D Appl. Phys.* 42 (2009) 095420.
- [28] M. Ahmad, E. Ahmed, Z.L. Hong, N.R. Khalid, W. Ahmed, A. Elhissi, Graphene-Ag/ZnO nanocomposites as high performance photocatalysts under visible light irradiation, *J. Alloy. Compd.* 577 (2013) 717–727.
- [29] N. Izu, K. Shimada, T. Akamatsu, T. Itoh, W. Shin, K. Shiraishi, T. Usui, Polyol synthesis of Al-doped ZnO spherical nanoparticles and their UV–vis–NIR absorption properties, *Ceram. Int.* 40 (2014) 8775–8781.
- [30] P. Kadam, C. Agashe, S. Mahamuni, Al-doped ZnO nanocrystals, *J. Appl. Phys.* 104 (2008) 103501.
- [31] O. Akhavan, R. Azimirad, S. Safa, Functionalized carbon nanotubes in ZnO thin films for photoinactivation of bacteria, *Mater. Chem. Phys.* 130 (2011) 598–602.
- [32] H. Fan, X. Zhao, J. Yang, X. Shan, L. Yang, Y. Zhang, X. Li, M. Gao, ZnO-graphene composite for photocatalytic degradation of methylene blue dye, *Catal. Commun.* 29 (2012) 29–34.
- [33] S.S. Alias, A.B. Ismail, A.A. Mohamad, Effect of pH on ZnO nanoparticle properties synthesized by sol-gel centrifugation, *J. Alloy. Compd.* 499 (2010) 231–237.
- [34] I.Y.Y. Bu, Highly conductive and transparent reduced graphene oxide/aluminium doped zinc oxide nanocomposite for the next generation solar cell applications, *Opt. Mater.* 36 (2013) 299–303.
- [35] S. Pan, X. Liu, ZnS-Graphene nanocomposite: synthesis, characterization and optical properties, *J. Solid State Chem.* 191 (2012) 51–56.
- [36] A. Wei, L. Xiong, L. Sun, Y. Liu, W. Li, W. Lai, X. Liu, L. Wang, W. Huang, X. Dong, One-step electrochemical synthesis of a graphene-ZnO hybrid for improved photocatalytic activity, *Mater. Res. Bull.* 48 (2013) 2855–2860.
- [37] W. Han, L. Ren, X. Qi, Y. Liu, X. Wei, Z. Huang, J. Zhong, Synthesis of CdS/ZnO/graphene composite with high-efficiency photoelectrochemical activities under solar radiation, *Appl. Surf. Sci.* 299 (2014) 12–18.